

## Single Molecule Dynamics Studied by Polarization Modulation

T. Ha, Th. Enderle, and D. S. Chemla

*Physics Department, University of California at Berkeley, Berkeley, California 94720  
and Molecular Design Institute, Materials Sciences Division, Lawrence Berkeley National Laboratory,  
1 Cyclotron Road, Berkeley, California 94720*

P. R. Selvin

*Life Science Division, Lawrence Berkeley National Laboratory, 1 Cyclotron Road, Berkeley, California 94720*

S. Weiss

*Molecular Design Institute, Materials Sciences Division, Lawrence Berkeley National Laboratory, 1 Cyclotron Road,  
Berkeley, California 94720*

(Received 1 May 1996; revised manuscript received 9 July 1996)

We observed and made unambiguous distinctions between abrupt photophysical events of single molecules: a rotational jump of a single dipole, a transition to a dark state (reversible and irreversible photobleaching), and a spectral jump. The study was performed in the far field by modulating the excitation polarization and monitoring the fluorescence in time. This technique also allowed us to measure the in-plane dipole orientation of stationary single molecular dipoles with subdegree accuracy and to resolve desorption and readsorption of fluorophores from and onto a glass surface. In one case, clear evidence was obtained for rapid rotation of the dipole after a desorption process. [S0031-9007(96)01623-7]

PACS numbers: 33.15.Kr, 33.50.-j, 33.80.-b

Recent advances in single molecule imaging and spectroscopy have made it possible to investigate individual molecular properties at ambient conditions. Diffusing single molecules have been detected in water streams [1], water drop [2], and fluid lipid membranes [3]. Immobilized molecules have been detected and imaged with the near-field scanning optical microscope (NSOM) [4–9] and in the far field both by confocal microscopy [10] and wide-field microscopy [11–13]. Moreover, single molecule emission spectra [5,14], excitation spectra [15], lifetime [6–10] and resonance energy transfer between two single molecules [14] have been measured.

Possibilities for utilizing single molecule imaging and spectroscopy to biological applications have been demonstrated [11–13,16,17]. Before such applications can be realized, single fluorophore dynamics has to be characterized under the appropriate conditions. In this paper, we present a convenient method both for monitoring dynamical events with good time resolution and for distinguishing among different phenomena in the emission of single fluorophores.

Güttler *et al.* used polarization modulation in excitation spectroscopy of pentacene molecules in *p*-terphenyl [18]. Xie *et al.* modulated the polarization between two discrete values ( $0^\circ$  and  $90^\circ$ ) to rule out dipole rotation as the origin of abrupt emission jumps in sulforhodamine 101 adsorbed on glass [6]. In this work, we excite single molecules in the far field with linearly polarized light which is continuously modulated, on a millisecond time scale, in polarization angle. The fluorescence of the molecules is then detected in time. We measured the in-plane

component of a single dipole with great accuracy, and distinguished between spectral jumps, transitions to dark states, and orientational effects. In particular, we used the technique to study dipole rotation of fluorophores linked to a short single strand DNA (ssDNA) molecule which was attached to a silanized glass surface. We resolved desorption and readsorption of fluorophores from and onto the surface, resulting in rotational jumps.

A 514 nm laser beam was introduced through the epillumination path of a fluorescence microscope and the polarization was modulated with an electro-optic modulator. The resulting linear polarization (modulated in time) at the sample plane was better than 100 to 1. The detection scheme is described elsewhere [14]. A 10 nM buffer solution of Texas Red (TR) or tetramethylrhodamine (TMR) molecules, covalently bound to ssDNA molecules (20 base pairs long), was prepared [14]. 1  $\mu$ L of the solution was spread on HF cleaned and aminopropylsilane treated glass coverslip and then immediately washed with water to remove the remaining salt. The resulting areal concentration of fluorescent molecules was less than  $0.5/\mu\text{m}^2$ .

Figure 1(a) shows an emission time trace (solid line) from a single TR-DNA molecule while the excitation polarization is repeatedly modulated from  $0^\circ$  to  $90^\circ$  (dotted line). The intensity of the emission signal  $F(t)$  is proportional to the absorption, which, according to the dipole approximation, is  $F(t) \propto |\vec{\mu} \cdot \vec{E}(t)|^2$  where  $\vec{\mu}$  is the molecular transition dipole and  $\vec{E}(t)$  is the laser field. The data acquired at each polarization sweep can therefore be fit with  $a \cos^2(x - b) + c$ , where  $x$  is the polarization angle,  $a$  is the signal intensity,  $b$  is the in-plane dipole

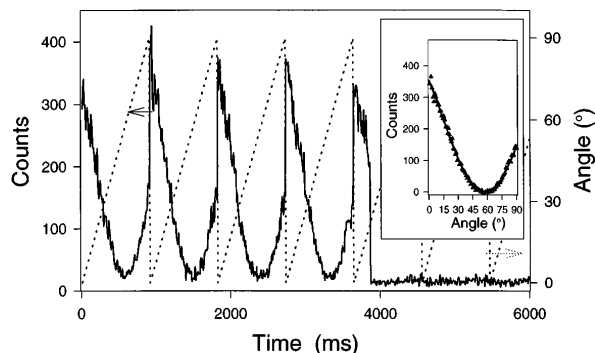


FIG. 1. Fluorescence time trace of a single TR molecule (solid line) and instantaneous excitation polarization angle (dotted line). Inset shows the averaged signal of the first four periods (filled triangles), and a fit to  $a \cos^2(x - b) + c$  (solid gray line).

angle, and  $c$  is the background. We found that fitting parameters to individual consecutive sweeps varied very little, indicating a fixed orientation of the dipole. To improve the accuracy, the fitting was done on an average of the first four periods [black triangles in Fig. 1(b)]. In the fifth period, the molecule photobleached. A best fit to the data is shown in solid gray line.

From the fit, we can extract the in-plane component of the dipole orientation with an accuracy of  $0.2^\circ$ . The accuracy varies from molecule to molecule. It depends on signal level (which depends on dipole orientation and spectral peak position). Other noise sources, such as spectral jumps, long dark states, and to a lesser extent short dark states [19], can limit the accuracy as well. Longer dark states and spectral jumps can strongly affect dipole orientation measurements if they occur on a time scale shorter than the full modulation period. In spite of the possible noise sources, emission from molecules with stationary dipoles could be fit with very good accuracy, due to the utilization of phase sensitive detection. Similar measurements were made on over 200 individual TR or TMR molecules. Most (over 97%) of the molecules showed stationary dipoles.

Figure 2(a) further supports this claim. It shows an emission time trace of a TMR molecule (solid line) which undergoes a transition to a dark state. The molecule stopped emitting light from 5.7 to 8 s in the scan [7]. The averages of the first 4 modulation periods before and the last 4 periods after the dark state are plotted in insets 3(b) and 3(c), respectively, along with curve fits. The data clearly demonstrate that the phase of the modulated signal is the same before ( $b = -42.8^\circ \pm 0.8^\circ$ ) and after ( $b = -41.3^\circ \pm 0.8^\circ$ ) the transition to the dark state. This shows that the dark period does not originate from a rotation, but from a transition to a nonemitting state or a large spectral jump.

Figure 3 is an example for a spectral jump, which can unambiguously be distinguished from dipole rota-

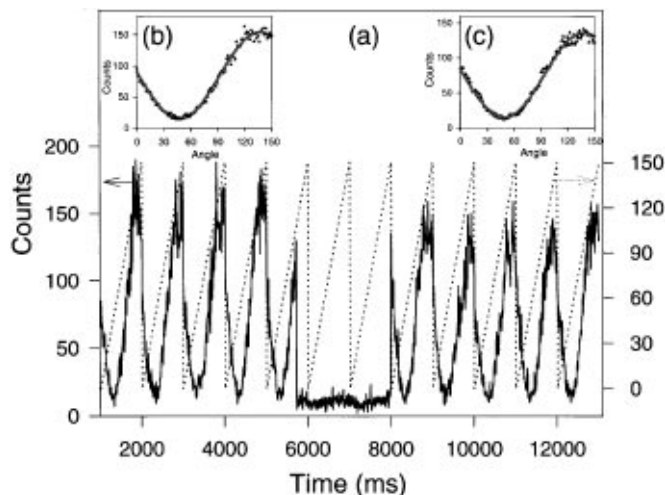


FIG. 2. (a) A transition to a dark state (2.3 s long) of a TMR molecule. The molecule photobleached after 51 s (not shown). The molecule maintained the same dipole orientation [from fits in insets (b) and (c)] throughout the transition to the dark state.

tion. The emission of a single TR molecule was separated by a dichroic mirror ( $\lambda_{\text{cutoff}} = 600 \text{ nm}$ ) and was simultaneously monitored in two channels while the excitation polarization was modulated. Figure 3(a) shows the two time traces, starting at scan #15. The signals on both channels were fit as in Fig. 1 for each modulation period. In Fig. 3(b), the ratio  $a_{\text{short}}/a_{\text{long}}$  (solid line, filled circles) is plotted as a function of the modulation period number. The phases of both signals, for each period,  $b_{\text{long}}$  and  $b_{\text{short}}$ , are plotted in black squares and gray triangles, respectively. In scan #24, the total emission from the molecule is increased threefold and the amplitude ratio is abruptly changed from 0.2 to 0.5, with no apparent change in the phase (and hence, no rotation). In general, a change in the counts ratio can come either from spectral changes or from reorientation of the dipole moment (see Fig. 5 below). This latter case is due to the strong polarization dependence of the dichroic mirror. While spectral jumps exhibit only a change in the relative intensity between the two channels, dipole reorientation exhibits a change in the phase of the modulated signal as well, as shown below, in Fig. 4. Therefore, the modulation technique can distinguish between spectral jumps and orientational effects. Since the dipole in Fig. 3 did not rotate, the data can only be explained by a spectral jump toward the blue. The inset of Fig. 3(b) illustrates the relative alignment of the absorption and emission lines before and after the spectral jump, the excitation laser wavelength, and the dichroic cutoff. The threefold increase in the total signal is due to the blueshift in absorption, which increases the absorption at the excitation wavelength, and hence the total emission. As the emission also blueshifts, the intensity in the short-wavelength channel increases more than in the long-wavelength channel, and therefore increases the ratio  $a_{\text{short}}/a_{\text{long}}$ .

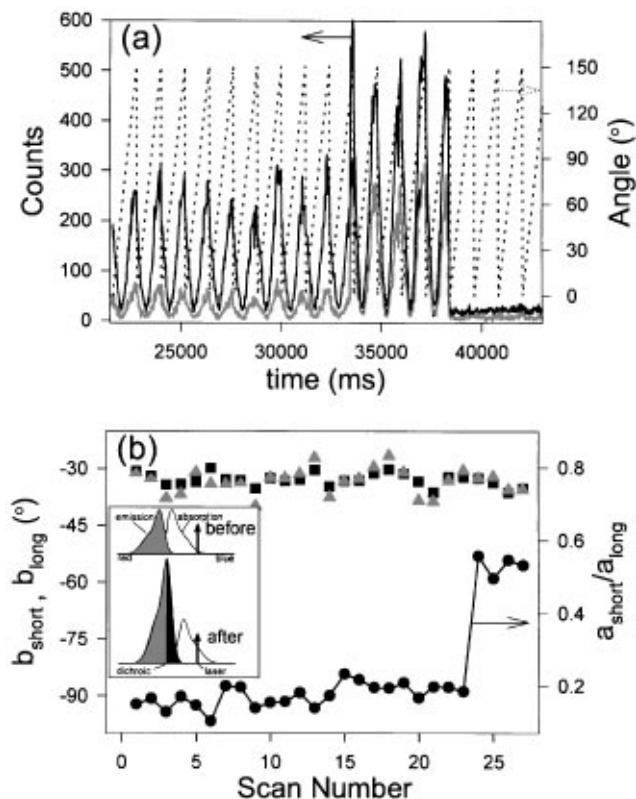


FIG. 3. (a) A spectral jump toward the blue of a TR molecule. Black line is the signal on the long-wavelength channel, and gray line is the signal on the short-wavelength channel. (Data from scan #1 to #14 are not shown.) (b) The data for each channel are fit for each polarization modulation period. The ratio  $a_{\text{short}}/a_{\text{long}}$  (solid black line, filled circles) and the phases of both signals,  $b_{\text{long}}$  and  $b_{\text{short}}$ , are plotted in black squares and gray triangles, respectively.

Moreover, by fully characterizing the response of the dichroic mirror for the typical emission spectrum of a single TR molecule, we could model and predict the ratio change for spectral jumps and/or dipole reorientation. This model allowed us to extract the peak position of the emission spectrum from the measured absorption dipole orientation and from the measured ratio between the two channels (here we assume that the absorption dipole and the emission dipole are closely aligned). By using this model for the data shown in Fig. 3, it was possible to conclude that the peak position of the emission spectrum jumped from 633 to 623 nm.

Out of more than 200 molecules examined, 5 molecules displayed rotational jumps that changed the dipole orientation. Figure 4(a) shows an emission time trace of a TR-DNA molecule, measured with a single detector. For the first 4 polarization scans, the dipole orientation is static. In the fifth scan, there is an interruption in the molecular emission. After the interruption, the emission signal resumes its initial value, but the phase changed. It was found that after the interruption, the molecule changed its in-plane orientation by  $7.5^\circ \pm 0.4^\circ$ . Because the peak

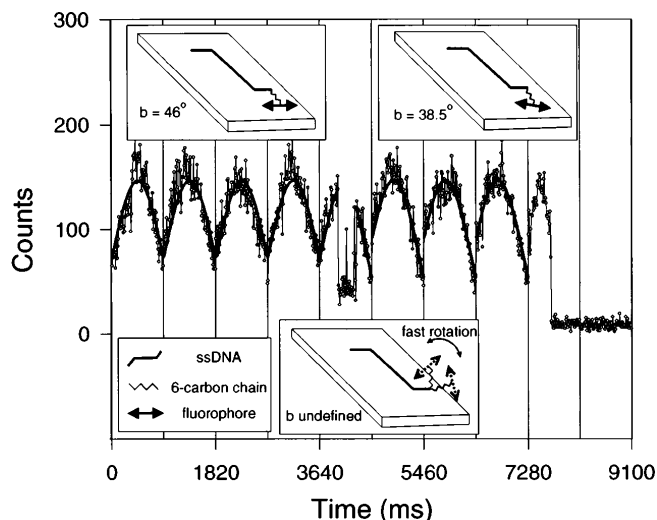


FIG. 4. A  $7.5^\circ$  in-plane rotational jump of a TR molecule. Solid line is the fit to the data before and after the interruption. Vertical lines separate each modulation period from 0 to 90 degrees. Insets show a model for the rotational jump.

intensity remained the same, we deduce that the out-of-plane dipole component did not change.

Similar to Fig. 4, all observed rotational jumps followed a transition period in the molecular emission (0.1 to 1.3 s long) that showed up as an interruption in the well behaved series of sinusoidal curves. The data shown in Fig. 5(a) was acquired with the two-color detection scheme, as in Fig. 3. The sum of the counts on the short- and long-wavelength channels from another TR-DNA molecule is shown (solid line, bottom curve). The molecular emission exhibits a sinusoidal signal in time, which is interrupted 3 times. The three transition periods (labeled "1," "2," and "3" in the figure) are characterized by noisy and unmodulated molecular emission. In these periods, the molecule has no stationary dipole. The signal in the stationary periods was fit and the dipole angle was extracted (noted in the figure). A change in dipole orientation followed each interruption in the emission. Also shown in Fig. 5(a) is the ratio between the two channels' counts (filled circles, top curve). For the stationary dipole periods, the ratio is fixed and featureless.

A likely explanation for the nature of the transition periods in Figs. 4 and 5 is desorption of the fluorophore from and reabsorption to the surface (see insets in Fig. 4). The treatment of the glass surface ensures the binding of the DNA. The fluorophore, linked to the DNA through a flexible 6-carbon chain, is most likely bound flat to the surface (near-field imaging of identically prepared samples revealed no  $z$  component of the dipole). However, if the fluorophore is only loosely bound to the surface, it can desorb from the surface and rapidly rotate along the linker, before it is reabsorbed at another site with different orientation. The desorption process might be thermally activated, if the binding energy to the surface

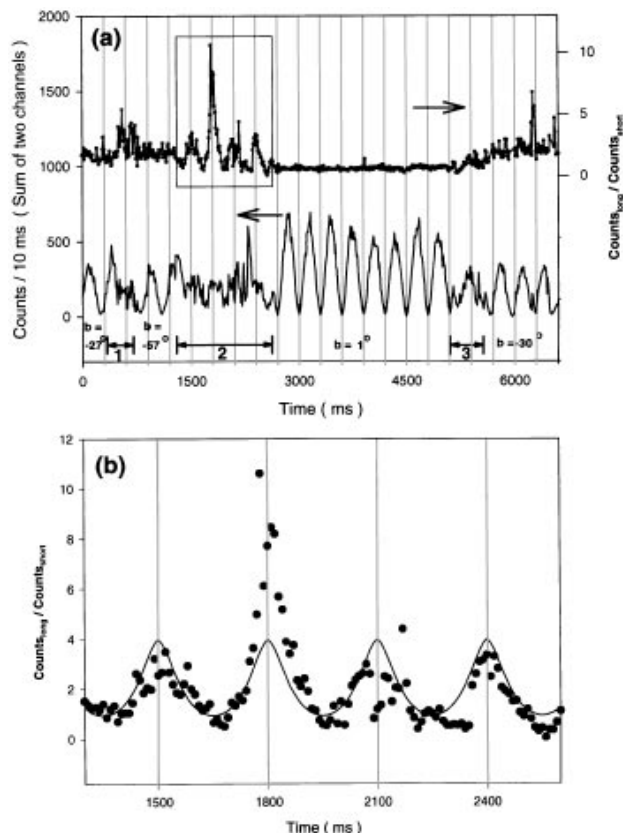


FIG. 5. (a) The ratio and sum of two channel counts from a single TR-DNA that shows multiple rotational jumps. The transition periods of three rotational jumps are marked with 1,2,3. Modulation was done from  $-81^\circ$  to  $81^\circ$  where  $0^\circ$  is when the excitation was  $s$  polarized with respect to the dichroic beam splitter. (b) Zoom-in to the boxed area in (a). Solid line is the fit under the assumption that the molecule rotates freely during the transition period.

is comparable to  $k_B T$ , or may be the result of a light induced process (such as conformational change of the molecule). The mechanism for desorption will be the subject of future investigations. When the fluorophore is free to rapidly rotate and sample many solid angles, the emission intensity is reduced, as clearly shown. A strong support for this model is obtained from the rich dynamics observed in the ratio signal during the transition periods. During transition period "2" [zoom-in in Fig. 5(b)], the ratio displays a clear modulation with the same period as the excitation polarization. Barring the unlikely possibility of spectral jumps exactly in phase with the excitation polarization, these data give evidence for rapid and free rotation of the fluorophore during the transition period. Free rotation on a time scale faster than the integration time (10 ms) but slower than radiative lifetime ( $\approx$ ns) will result in partially polarized

emission along the excitation polarization. Because of the polarization dependence of the dichroic mirror, the ratio signal between the two channels will follow the excitation polarization, and hence will be modulated with the same modulation period. Using the same model as in Fig. 3, and assuming full random rotation over all angles, the data in Fig. 5(b) were fit with a single fitting parameter—the spectral peak position, and the spectral peak position was determined to be 600 nm. Deviations from the fit are probably due to spectral jumps or hindered motions resulting from brief visits to loosely bound sites within the transition period.

We thank D. F. Ogletree for his help in data acquisition and software developments. This work was supported by the Laboratory Directed Research and Development Program of Lawrence Berkeley National Laboratory under U.S. Department of Energy, Contract No. DE-AC03-76SF00098 and by the Office of Naval Research, Contract No. N00014-95-F-0099.

- 
- [1] E. B. Shera *et al.*, Chem. Phys. Lett. **175**, 553 (1990).
  - [2] S. Nie, D.T. Chiu, and R.N. Zare, Science **266**, 1018 (1994).
  - [3] Th. Schmidt *et al.*, J. Phys. Chem. **99**, 17 662 (1995).
  - [4] E. Betzig and R.J. Chichester, Science **262**, 1422 (1993).
  - [5] J.K. Trautman, J.J. Macklin, L.E. Brus, and E. Betzig, Nature (London) **369**, 40 (1994).
  - [6] X.S. Xie and R.C. Dunn, Science **265**, 361 (1994).
  - [7] W.P. Ambrose, P.M. Goodwin, J.C. Martin, and R.A. Keller, Science **265**, 364 (1994).
  - [8] R.X. Bian, R.C. Dunn, X.S. Xie, and P.T. Leung, Phys. Rev. Lett. **75**, 4772 (1995).
  - [9] J.K. Trautman and J.J. Macklin, Chem. Phys. **205**, 221 (1996).
  - [10] J.J. Macklin, J.K. Trautman, T.D. Harris, and L.E. Brus, Science **272**, 255 (1996).
  - [11] T. Funatsu, Y. Harada, M. Tokunaga, K. Saito, and T. Yanagida, Nature (London) **374**, 555 (1995).
  - [12] I. Sase *et al.*, Biophys. J. **69**, 323 (1995).
  - [13] R.D. Vale, T. Funatsu, D.W. Pierce, L. Romberg, Y. Harada, and T. Yanagida, Nature (London) **380**, 451 (1996).
  - [14] T. Ha, Th. Enderle, D.F. Ogletree, D.S. Chemla, P. Selvin, and S. Weiss, Proc. Natl. Acad. Sci. U.S.A. **93**, 624 (1996).
  - [15] X.S. Xie (private communication).
  - [16] M. Eigen and R. Rigler, Proc. Natl. Acad. Sci. U.S.A. **91**, 5740 (1994).
  - [17] J.D. Harding and R.A. Keller, Trends Biotechnol. **10**, 55 (1992).
  - [18] F. Güttler, J. Sepiol, T. Plakhotnik, A. Mitterdorfer, A. Renn, and U.P. Wild, J. Lumin. **56**, 29 (1993).
  - [19] T. Ha *et al.* (to be published).